

Continuous-time random-walk simulation of H₂ formation on interstellar grains

Q. Chang¹, H. M. Cuppen¹, and E. Herbst²

¹ Department of Physics, The Ohio State University, Columbus, Ohio 43210, USA

² Departments of Physics, Chemistry, and Astronomy, The Ohio State University, Columbus, OH 43210, USA
e-mail: herbst@mps.ohio-state.edu

Received 12 August 2004 / Accepted 31 December 2004

Abstract. The formation of molecular hydrogen via the recombination of hydrogen atoms on interstellar grain surfaces has been investigated anew. A detailed Monte Carlo procedure known as the continuous-time random-walk method has been used. This Monte Carlo approach has two advantages over the stochastic master equation method: it treats random walk on a surface correctly, and it can easily be used for inhomogeneous surfaces. The recombination efficiency for H₂ formation as a function of surface temperature and grain size has been calculated for a variety of grain surfaces with a flux of hydrogen atoms representative of diffuse interstellar clouds. The surfaces studied include homogeneous olivine and amorphous carbon, characterized by single energies for the diffusion barrier and binding energy of H atoms, inhomogeneous versions of these two surfaces with distributions of H-atom diffusion barriers and binding energies, and a variety of mixed surfaces of olivine and carbon. For the homogeneous surfaces, we confirm that the temperature range for efficient formation of H₂ is very small. At temperatures near peak efficiency, there is little dependence on grain size. At temperatures higher than those of peak efficiency, the Monte Carlo procedure exhibits smaller efficiencies for molecular hydrogen formation than the master equation method in the limit of large grain sizes. For various types of inhomogeneous and mixed surfaces, the major effect we find is an increase in the temperature range over which the efficiency of molecular hydrogen formation is high. Efficient formation of H₂ in diffuse interstellar clouds now seems possible with inhomogeneous grains.

Key words. astrochemistry – ISM: abundances – ISM: molecules – molecular processes

1. Introduction

Hydrogen is the most abundant element in the universe and, not surprisingly, molecular hydrogen, the simplest molecule formed from hydrogen atoms, has been found to be the most abundant molecule. Moreover, the existence of molecular hydrogen leads to the subsequent formation of the molecular ion H₃⁺ in interstellar clouds, which in turn leads to a rich gas-phase chemistry that produces many of the over one-hundred molecules detected in the interstellar medium (Duley & Williams 1984; Williams 1998; Herbst 2001). Ironically, however, the gas-phase production of molecular hydrogen from atoms cannot occur efficiently in the interstellar medium (Gould & Salpeter 1963), and it has been known for some time that molecular hydrogen in the ISM must be produced on dust grains.

The exact mechanism or mechanisms by which molecular hydrogen is formed on the surfaces of cold dust particles is still a matter of considerable conjecture today. Following the work of Watson & Salpeter (1972), Pickles & Williams (1977), Tielens & Allamandola (1987), Hasegawa et al. (1992) and others, astronomers have focused on a low-temperature version of the so-called Langmuir-Hinshelwood mechanism, in

which gaseous H atoms land on cold grain surfaces and bind via weak forces in a process known as “physisorption”. The binding occurs preferentially in sites corresponding to potential wells, with barriers separating these wells. The weakly-bound hydrogen atoms are able to diffuse on the grains by thermal hopping over the barriers and possibly tunneling under them. Molecular hydrogen is formed without activation energy when two hydrogen atoms reach the same site. Opposing this process is the desorption of hydrogen atoms from a grain surface, which can occur via thermal evaporation or some non-thermal means, such as cosmic ray-induced sputtering or quasi-thermal excitation. The formation of molecular hydrogen via the Langmuir-Hinshelwood mechanism on grains should then occur efficiently over a limited temperature range defined in the following manner.

The lower limit of the temperature range is reached when the H atoms move so slowly that molecular hydrogen cannot be formed diffusively. This lower limit is strongly affected by whether quantum tunneling can occur between sites; if tunneling is efficient, then even at the lowest temperatures H-atom diffusion can occur, whereas if the dominant process is classical thermal hopping, the diffusion rate is exponentially

sensitive to temperature. Indeed, if tunneling is efficient, the lower limit may be more appropriately defined by the inability of the molecular hydrogen product to evaporate from the grain surface. The upper limit of the temperature range occurs when desorption becomes more rapid than diffusion, so that H atoms do not remain on grains long enough to react. At temperatures sufficiently low that diffusion cannot occur, if they exist, another process, known as the Eley-Rideal mechanism, can dominate the production of molecular hydrogen. In this mechanism, hydrogen atoms on the surface are bombarded by gas-phase atoms. To complicate matters further, it is entirely possible that adsorbing hydrogen atoms can bind with differing amounts of binding energy depending on the details of the surface site. A relatively simple example is a binary system in which both weak binding (physisorption) and strong binding (chemisorption) occur (Cazaux & Tielens 2004). A possible result is that efficient H₂ formation can occur over a wide range of temperatures. More complex scenarios are also possible, especially for poorly characterized surfaces. For example, there can exist complete distributions of surface binding and diffusion energies, depending on the frequency with which certain types of sites and defects occur. The temperature distribution over which molecular hydrogen formation is efficient on these complex surfaces has not yet been studied theoretically.

In a heartening development, the formation of molecular hydrogen has recently been studied in several laboratories on a variety of cold surfaces representative of the interstellar medium. The group of Vidali et al. studied the process via temperature-programmed desorption (TPD) of HD on olivine and amorphous carbon (Pirronello et al. 1997a,b, 1999), and via TPD of HD, H₂, and D₂ on amorphous ice (Roser et al. 2002), while Hornekaer et al. (2003) studied H₂ formation on “amorphous solid water” (ASW). The Vidali et al. experiments on the first two surfaces were analyzed by Katz et al. (1999), who found that the results could be fit by a simple Langmuir-Hinshelwood mechanism with single binding energies for H atoms and H₂ molecules on each surface as well as single barriers for H-atom diffusion. In addition, they found no evidence for tunneling from site to site. With this analysis, Katz et al. (1999) estimated that, under interstellar conditions, the formation of molecular hydrogen will only occur efficiently around a very narrow temperature range. For olivine grains, for example, this range occupies a few K only in the vicinity of 8 K for diffuse clouds (Biham et al. 2001), while for amorphous carbon it occurs in the vicinity of 13 K. The formation of H₂ on amorphous low-density ice appears to be more complex; a recent analysis of the experimental data of Roser et al. (2002) by Perets et al. (2004) shows that the molecular hydrogen *product* appears to have three different binding energies with distributions of unstated width. Indeed, a detailed analysis of the TPD data shows that under interstellar conditions, H₂ formation is efficient in a somewhat broader range – 14–20 K – when one considers both low-density and high-density ices (Perets et al. 2004). Of course, formation of molecular hydrogen on ice is not relevant to the diffuse cloud problem, since ice monolayers do not develop until a considerable extinction exists.

The detailed interpretation and results of the Vidali et al. experiments have been challenged by two sources. The first

challenge comes from Cazaux & Tielens (2004), who used a more complex model to analyze the olivine and carbonaceous data of Vidali et al. than did Katz et al. (1999). This model was also used to simulate high-temperature H₂ formation on graphite (Zecho et al. 2002). In particular, Cazaux & Tielens (2004) included both physisorption and chemisorption binding sites, as well as quantum mechanical tunneling and thermal hopping between sites. They also treated H and D atoms as distinct entities, whereas Katz et al. (1999) did not. Unlike the analysis of Katz et al. (1999), these authors found that molecular hydrogen can be formed over a wide temperature range even if the surface can be characterized simply in terms of just two binding energies. At lower temperatures, recombination is dominated by reactions between physisorbed and chemisorbed atoms, whereas at higher temperatures (up to 500 K), chemisorbed atoms become mobile and dominate the Langmuir-Hinshelwood kinetics. The result is of astronomical importance because it is clear that H₂ formation should occur over a wide range of surface temperatures, from lows of 10 K and under in dense cold clouds, through temperatures of 15–25 K in diffuse clouds (Li & Draine 2001), to even higher temperatures in photon-dominated regions. The result relies on the uncertain ability of H atoms to access chemisorbed states through precursor physisorbed states without a cripplingly large activation energy. Accessing chemisorption sites directly is another possibility, but, at least for graphite, theoretical results indicate the existence of an activation energy of ≈ 0.2 eV for direct sticking of a gas-phase H atom into a chemisorption site, caused partially by surface reconstruction effects (Zecho et al. 2002; Sha & Jackson 2002). Experimental TPD results on this system (Zecho et al. 2002) involve H and D atoms generated in a 2000 K source.

Posing another challenge, the recent experiments by Hornekaer et al. (2003) on amorphous solid water show that molecular hydrogen is formed efficiently at even the lowest temperatures sampled by the group (8 K), indicating a high mobility for hydrogen atoms possibly due to tunneling. There is little temperature dependence of the results. The picture of these authors is that hydrogen recombination occurs efficiently inside the porous structure of the ASW at even the lowest temperatures studied, and that evaporation eventually but not immediately follows.

Even if one assumes that the formation of molecular hydrogen on surfaces occurs simply; i.e., by classical (thermally-activated) diffusion, or hopping, on a surface such as olivine or amorphous carbon correctly characterized by one binding energy and one diffusion barrier for H atoms, there is still the problem of determining the rate of the process on interstellar dust grains. Unlike the laboratory surfaces used, dust grains are small and, given the low density of interstellar gas, do not have sizeable numbers of reactant atoms on their surfaces at any given time. Indeed, under a variety of interstellar conditions and for a variety of grain sizes, the average number of H atoms per grain is likely to be unity or less (Tielens & Hagen 1982; Biham et al. 2001; Lipshtat et al. 2004). Under such circumstances, the standard rate equations used in surface science (Hasegawa et al. 1992; Biham et al. 2001), which are quite

analogous to gas-phase equations, may not be applicable both due to the discreteness of the number of H atoms per grain and the significant fluctuation around the mean value. These deficiencies in the rate method for surface chemistry were first presented in the astronomical literature by Tielens & Hagen (1982) and restated in a well-known talk by Tielens (unpublished) at a March 1995 conference in Leiden, The Netherlands. Since that time, several methods to study surface chemistry on interstellar grains in a more appropriate manner have been suggested. The more rigorous methods involve two stochastic approaches to the problem: a Monte Carlo method first utilized by Charnley (2001) and a master equation treatment introduced independently by Biham et al. (2001) and Green et al. (2001). For detailed discussions of the methods, see Stantcheva et al. (2002) and Biham & Lipshtat (2002). Although both of these approaches can be used to study the formation of molecular hydrogen on grains, only the latter seems to be usable for a combined gas-grain model of interstellar clouds with large numbers of both gas-phase and grain-surface reactions (Stantcheva & Herbst 2004). In addition to the stochastic approaches, there is a simpler and semi-empirical method, known as the modified rate equation (Caselli et al. 1998, 2002), in which the classical rate equations are modified to take into account, at least partially, the discreteness of the surface chemistry problem. The modified rate method is in standard use for models with large gas-grain reaction networks (Roberts & Herbst 2002), but progress in the master equation method has been such to generate optimism that it will be usable in the near future (Stantcheva & Herbst 2004; Lipshtat & Biham 2004).

Both stochastic methods should yield the same results as do classical rate equations in the limit of significant numbers of species on grains. This asymptotic result has been shown to occur for the formation of H₂, HD, and D₂ on grains of a variety of sizes (Biham et al. 2001; Lipshtat et al. 2004). Although the stochastic approaches currently in use differ in their results from rate equations in the limit of a small number of reactive species per grain, these approaches still incorporate an approximation that may lead to error. The reasons for the possible error have been studied in some detail in the statistical physics literature (Lin et al. 1996; Hinrichsen 2000; Krug 2003; Lindenberg et al. 1995; Weiss & Rubin 1983; Simon 1995), but for our purposes here, one can simplify the problem in the following manner. The basic common assumption to the previous methods utilized is that the rate of reaction is determined by the rate of hopping (or tunneling) of a hydrogen atom from one site to a nearest neighbor site multiplied by the probability of finding a reactant partner in this site. This is clearly an average treatment only: on any given grain the reactant partner is likely to lie more than one nearest-neighbor site away. A more detailed treatment should investigate the actual distribution of reactive particles on a given grain and how they move about the surface as a function of time. In other words, to simulate a stochastic process in two dimensions exactly, one must keep track of where each reactant particle is and where it goes. The type of motion undergone by the particles is known as a “random walk”. In two dimensions, the number of nearest neighbor sites is relatively small, so that during their random walk, particles have a significant probability to jump back to sites occupied previously,

a phenomenon known as “back diffusion”. Thus, the actual number of different sites visited during a random walk is smaller than the number of hops from site to site. How important this effect is for the rate of reaction must be determined by detailed calculation although it has been shown that the inefficiency of random walking reduces the rate under most circumstances. Although the chemical master equation employed by Biham et al. (2001) and Green et al. (2001) does not consider random walk explicitly, the approach can be modified to include this correction (Montroll & Weiss 1965; Krug 2003; Bedeaux et al. 1971). Master equations with this modification are not easy to solve with the exception of very simple systems.

Besides the problems we have discussed above for the rate equation approach to surface chemistry and even for the two stochastic methods heretofore used to replace it, there is a limitation to the types of systems that can be studied by all of these methods. In particular, none of them can be used to treat a surface that is inhomogeneous, in the sense that adatoms experience a continuous range of differing binding energies and barriers against diffusion. This objection is not true for surfaces with a discrete number of differing energies; Cazaux & Tielens (2004) treated physisorbed and chemisorbed H atoms as two different species, and were able to use rate equations. If the desorption energy and diffusion barrier are not discrete but belong to a continuous distribution, however, as theoretical calculations for an amorphous ice surface (Buch & Czerminski 1991) suggest, it would be impossible to use the methods discussed exactly because we would have an infinite number of equations. Nevertheless, it is possible to approximate continuous distributions by numbers of discrete and closely spaced energies (Perets et al. 2004).

To eliminate the above problems and limitations as they relate specifically to the formation of molecular hydrogen, we have chosen to use the continuous-time random-walk (CTRW) Monte Carlo simulation method (Montroll & Weiss 1965) to model the formation of molecular hydrogen on grain surfaces. Instead of solving equations for surface abundances (rate equations) or probabilities (master equations), CTRW considers the actual hopping of a discrete number of H atoms from one site to another. Since diffusion, adsorption, and evaporation are treated with a Monte Carlo algorithm, fluctuations in population are considered automatically. Unlike previous Monte Carlo methods (Tielens & Hagen 1982; Charnley 2001), we take into account the actual position of H atoms so that the spatial distribution is also included in the simulation. Moreover, the number of nearest neighbors can easily be varied to check on the role “back diffusion” may play in reducing the rate of reaction. Finally, the method can readily be extended to inhomogeneous systems, which are more likely to be representative of interstellar grain surfaces and which may show effects not previously considered.

Using the CTRW approach, we report a study of the formation of molecular hydrogen under diffuse cloud conditions on a variety of grain surfaces of varying sizes and over a range of temperatures. Our principal goals are to determine if significant errors have been made in previous treatments of homogeneous grains, and to determine whether or not the use of inhomogeneous grains has a strong effect on the efficiency of

hydrogen formation. The rest of this paper is divided as follows. In Sect. 2, we introduce the continuous-time random-walk model and discuss the astronomical context, while in Sect. 3, we show and discuss results pertaining to the formation of H_2 on olivine, amorphous carbon, and mixtures of olivine and amorphous carbon. Our conclusions are presented in Sect. 4.

2. The model

2.1. CTRW approach

In the CTRW approach, H atoms are deposited on a grain lattice. We consider physisorbed H atoms only, and, following the analysis of Katz et al. (1999), assume that these atoms “hop” from site to site when they have enough energy to overcome a barrier against classical diffusion, a process known as “thermal activation”. With this assumption, we neglect quantum mechanical tunneling from site to site. The probability of hopping to each nearest site is assumed to be the same. If the H atom hops to a site that is already occupied by another H atom, H_2 is formed and released into the gas immediately. In the analysis of Katz et al. (1999), the fit to the experimental TPD results on olivine and amorphous carbon yielded a non-zero parameter labeled μ , which represents the fraction of H_2 molecules that are not ejected immediately, but remain on the grain until they evaporate. Our assumption that $\mu = 0$ is not important because, except at very low temperatures, H_2 will evaporate quickly if not immediately ejected. We neglect the deposition of additional H_2 molecules from space for the same reason and also since we are interested in forming H_2 in environments where it does not constitute a dominant fraction of the gas phase.

In total, there are four types of processes that occur in our model: the formation of H_2 , and the deposition, hopping, and desorption of H atoms. Deposition, hopping, and desorption are all Poisson processes, which means that they are memoryless, or Markovian. For a Poisson process the time interval t between two consecutive events follows an exponential distribution, which we will call a waiting-time distribution (WTD), and is given by the expression

$$\psi_a(t) = b_a \exp(-b_a t), \quad (1)$$

where b_a is the rate of process a , and b_a^{-1} is the average time in between events a . Waiting times WT_a are chosen by calling random numbers according to the standard prescription

$$WT_a = -\frac{\ln X}{b_a}, \quad (2)$$

where X is a random number, $0 < X < 1$.

For deposition, which we label process 0, $b_0 = t_0^{-1}$ is the deposition rate of H atoms (in units of atoms s^{-1}) and t_0 is the average deposition time. For hopping (process 1), b_1 is the hopping rate and has the same form as that used in the rate and master equation approaches:

$$b_1 = \nu \exp(-E_b/T), \quad (3)$$

where E_b (in units of K) is the diffusion barrier, T is the surface temperature, and ν is the attempt rate, which we choose to be

$10^{12} s^{-1}$ to compare with previous work (Biham et al. 2001). Desorption is considered to be another independent Poisson process, with the same type of WTD for a single desorption energy and a desorption rate given by

$$b_2 = \nu \exp(-E_D/T), \quad (4)$$

where E_D is the desorption energy. If hopping and desorption are independent, the distributions can be multiplied and renormalized to obtain a total WTD for desorption and hopping of the form

$$\psi(t) = b \exp(-bt) \quad (5)$$

with a total rate

$$b = b_1 + b_2. \quad (6)$$

The competition between desorption and hopping can then easily be simulated (Gillespie 1976) by comparing the ratio of an individual rate to the total; e.g., $(b_2)/(b_1 + b_2)$, with a random number X . If X is smaller than the ratio, then the H atom will undergo desorption, otherwise it will hop.

For all H atoms on the surface, the time at which they will make their next move, either hopping or evaporation, is determined as described above. In addition, the next time at which a deposition occurs is similarly determined. All these times are compared and the processes are evaluated in the order of occurrence.

Whenever a hydrogen atom hops to another site or a new hydrogen atom arrives on the lattice, a new waiting time is generated for its next move. The actual clock time at which the move occurs is the current time plus the waiting time. Incoming H atoms are assigned random sites, and if there are H atoms already on the sites, the landing species will be bounced off. This effect corresponds to the Langmuir-Hinshelwood rejection term in rate equations. The sticking probability is otherwise assumed to be unity. Whenever an H atom arrives, the arrival time for the next H atom is generated randomly from the distribution $\psi_0(t)$.

We employ periodic boundary conditions in the simulation. The periodic boundary conditions are reasonable for grain surfaces because an H atom can always come back to where it started hopping by proceeding straight in a given direction.

After running for some time, a “steady-state” condition is reached in which the surface population of H atoms fluctuates around a constant value. Specific calculated times necessary to reach steady state range from 10^3 – 10^8 s. After steady state has been reached, we keep a continuous count of the number of arriving H atoms, N_H , and the number of H_2 molecules formed, N_{H_2} , and define a recombination efficiency η by the expression

$$\eta = \frac{2N_{H_2}}{N_H}. \quad (7)$$

We run the program a sufficiently long time that many H atoms arrive and the statistical noise is low.

2.2. Lattices, flux, and grains

We assume that the binding sites on an interstellar grain form a regular square lattice on which each site has either four nearest

neighbors, as in an fcc[100] plane, or six nearest neighbors, as in an fcc[111] plane. We will call the first case a type-1 lattice and the second a type-2 lattice. Hydrogen atoms strike an individual grain with a flux f_H in ML s^{-1} given by the expression (Biham et al. 2001)

$$f_H = \frac{v_H n_H}{4s} \quad (8)$$

where the initials “ML” stand for “monolayer”, v_H and n_H are the average velocity and density of H atoms, while s is the density of surface sites. The factor of 4 refers to spherical grains; with this formula, the deposition rate b_0 in units of atoms s^{-1} is given by

$$b_0 = 4\sigma_{gr} s f_H, \quad (9)$$

where σ_{gr} is the granular cross section (Biham et al. 2001). Following Biham et al. (2001), we utilize a flux representative of diffuse interstellar clouds for H atoms onto each grain of 1.8×10^{-9} ML s^{-1} .

Our chosen lattice sizes, ranging from 100 to 1.0×10^6 sites, can be related to spherical grain sizes via the relation

$$S = \pi d^2 s, \quad (10)$$

where S is the number of sites, and d is the diameter of the grain. As an example, with the experimentally derived surface site density of 2×10^{14} cm^{-2} for homogeneous olivine (Biham et al. 2001), our olivine grains with 10^5 lattice sites (316×316) possess a diameter of ≈ 0.13 μ , near the “standardly” chosen size. Our smallest grains, with 100 sites, similarly have diameters of 4 nm.

In this paper, we restrict consideration to bare surfaces of relevance to diffuse interstellar clouds. The problem of H_2 formation on ice is more of a dense cloud problem, and one that we do not treat here. The types of surfaces to be studied include (i) “homogeneous” olivine and amorphous carbon, both of which are assumed to possess a single binding energy and diffusion barrier for H atoms, as obtained by Katz et al. (1999); (ii) modified, or “inhomogeneous”, olivine and amorphous carbon surfaces in which binding energies and diffusion barriers for H atoms follow continuous distributions; and (iii) grains that are composed of mixtures of homogeneous olivine with homogeneous amorphous carbon, and of homogeneous olivine with inhomogeneous amorphous carbon. In the mixtures, both randomly placed individual carbon atoms and clusters of carbon atoms known as islands are studied. The more complex surfaces are treated because they are more realistic, and because the homogeneous surfaces, as treated by previous methods, show high efficiencies of molecular hydrogen formation in diffuse clouds only over astronomically unreasonable small ranges of temperature of a few K.

2.3. Distributions

Because we do not really know the actual shapes of the distributions, we include two possibilities. Let us first consider an exponential distribution. Defining the diffusion barrier E_b (in units of K) by the relation

$$E_b = E_{b0} + \Delta E_b, \quad (11)$$

we can write a distribution for ΔE_b of the form

$$f(\Delta E_b) = (T_0)^{-1} \exp\left(-\frac{\Delta E_b}{T_0}\right), \quad (12)$$

where T_0 is the average of ΔE_b , and the average diffusive barrier \overline{E}_b is equal to the sum of E_{b0} and T_0 .

We also study the case of a Gaussian distribution. For the diffusive case, the distribution can be written as

$$f(E_b) = \frac{1}{\sqrt{2\pi(T_0)^2}} \exp\left(-\frac{(E_b - \overline{E}_b)^2}{2(T_0)^2}\right) \quad (13)$$

where T_0 is the standard deviation and \overline{E}_b is the average diffusive barrier. An actual calculation of diffusive barrier and binding energy distributions for H atoms on amorphous ice clusters shows shapes that are more complex than either distribution considered here (Buch & Czerminski 1991).

Once a type of distribution and a measure of its width are chosen, we determine randomly a value of E_b for each lattice site. These energies are then used in the CTRW calculations to calculate waiting times. For small grains, especially, a number of different lattices must be used to develop proper statistics. Eventually, as grains become sufficiently small, they can be regarded as individual molecules with unique properties that should not be averaged. Because the desorption energy is generally correlated with the diffusion barrier (the stronger the binding, the higher the barrier to diffusion), we keep the ratio of diffusion barrier to desorption energy to be the same as that in the single barrier and desorption energy case. Thus, only one energy distribution need be used.

3. Results and discussion

3.1. Homogeneous olivine and amorphous carbon surfaces

Before analyzing the recombination efficiency for H_2 formation on more complicated surfaces, we would like to compare our results with those obtained by Biham et al. (2001) for the two homogeneous surfaces – olivine and amorphous carbon. We discuss the olivine case first and in some detail. In the earlier results, which were obtained using both the master equation and rate equation approaches, Biham et al. (2001) calculated the recombination efficiency at various temperatures as a function of grain size. To facilitate a comparison with their results, we will use the same parameters they used: an H-atom diffusion barrier of 287 K and a desorption energy of 373 K (Katz et al. 1999).

Figure 1 shows the calculated recombination efficiency η as a function of the number of sites on an olivine grain at 10 K. The circles are for a type 1 lattice (four nearest neighbors) while the squares are for a type 2 lattice (six nearest neighbors). The analogous calculated points of Biham et al. (2001) for η , obtained from the master equation approach and taken from their Fig. 3, are shown as diamonds by converting their abscissa of grain diameter to the number of sites S . Unlike the rate equation method, which yields a result totally independent of size, both the CTRW and master equation approaches show

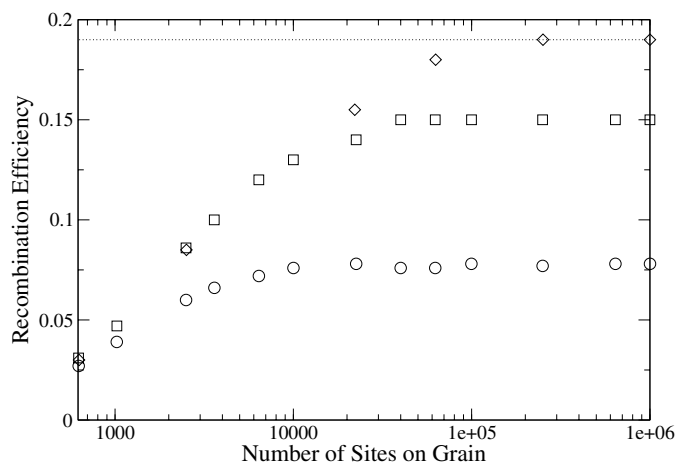


Fig. 1. Recombination efficiency as calculated by the CTRW approach on a homogeneous olivine surface at 10 K as a function of the number of grain sites. The circles represent results for a type 1 lattice while the squares are for a type 2 lattice. Previous results from Biham et al. (2001) with the master equation and rate equation approaches are also included as diamonds and a dotted line, respectively.

a size dependence. It can be seen in Fig. 1 that the agreement between the two approaches is reasonable but not perfect. If we start by comparing bigger grains, we see that the asymptotic value of 0.19 obtained by Biham et al. (2001) (which is also the value obtained by the rate equation method for all granular sizes) is larger than our values, which are 0.078 and 0.15 for type 1 and 2 lattices, respectively. The increase in efficiency with increasing number of nearest neighbors suggests, but does not prove, that in a treatment where random walk is included explicitly, diffusion is more effective when it is less likely that H atoms revisit sites previously accessed. Neither the rate equation nor the master equation approach includes random walk explicitly, but both approaches appear to mimic a limit in which back diffusion does not occur.

Now let us consider smaller grains. Here, the master equation results of Biham et al. (2001) show lower efficiencies than the asymptotic result, corresponding to the regime where the average population of hydrogen atoms per grain is less than unity. Interestingly, the recombination efficiency on small grains with our model agrees well with master equation results. As the grain size decreases, the master equation result decreases more strongly than the CTRW results. For a grain of diameter 10^{-6} cm corresponding to one with 624 lattice sites, the two methods are in excellent agreement: η determined via the master equation method is ≈ 0.03 while our results are 0.027 (type 1) and 0.031 (type 2). In these small grain simulations, the dominant factor for recombination is whether or not the grain can capture another H atom before the one present evaporates, because H atoms can quickly sweep over the surface even if diffusion in the CTRW calculations is not as efficient as in the master equation approach.

Under the diffuse cloud conditions chosen, previous treatments show that homogeneous olivine has only a small temperature range in which molecular hydrogen formation is efficient. It is interesting to see if the same effect occurs with the CTRW approach. Figure 2 shows our computed

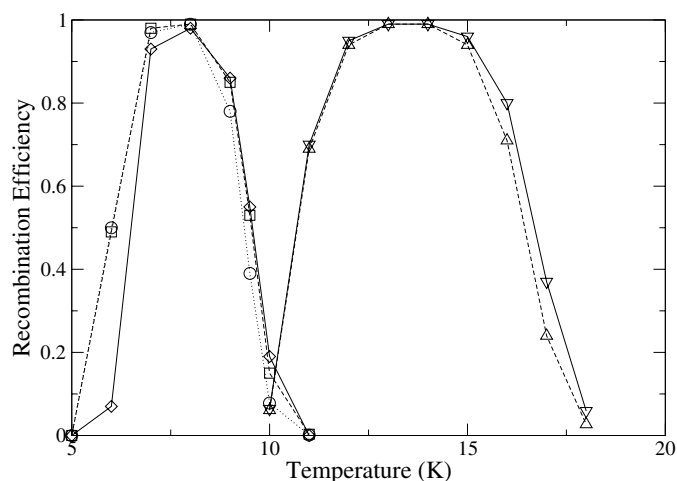


Fig. 2. Recombination efficiency as calculated by the CTRW approach for standard grains of homogeneous olivine and amorphous carbon as a function of surface temperature. For olivine, the circles represent a type 1 lattice while the squares represent a type 2 lattice. For carbon, the triangles pointed upwards and downwards represent, respectively, type 1 and 2 lattices. The master equation/rate equation results of Biham et al. (2001) for olivine are shown as diamonds.

recombination efficiency vs. surface temperature for type 1 and type 2 lattices for a grain of size $316 \times 316 \approx 10^5$ sites, a size that will henceforth be labeled “standard”. As a comparison, we also include the results by Biham et al. (2001). It can be seen that our results are in qualitative agreement with those of Biham et al. (2001), here showing only a very narrow temperature range (6–9 K) of high efficiency. The methods are in particularly good agreement when the efficiencies are at their highest, but differ somewhat at lower and higher temperatures. For example, by 10 K, as also seen in Fig. 1, our results are somewhat lower. Our calculated efficiency at 6 K, on the other hand, is somewhat greater than previous results because we ignore the existence of surface H_2 , which may be important at this low temperature. Unlike the situation at 10 K, there is little size dependence when the efficiency is high because H atoms remain on grains long enough that they collide with other surface H atoms even at very low striking rates per grain.

Another surface for which homogeneous parameters are available is amorphous carbon, analyzed by Katz et al. (1999). These authors derived a diffusive barrier for atomic H of 511 K and a desorption energy of 658 K. The larger values, compared with homogeneous olivine, suggest that molecular hydrogen formation on amorphous carbon will be efficient at higher temperatures than for olivine. Indeed, since both the barrier to diffusion and the desorption energy derived for amorphous carbon are approximately 1.77 times that of olivine, a more detailed assertion can be made. In particular, based on the forms of the rate parameters for diffusion and desorption, in which energies are divided by the temperature, the recombination efficiency for carbon vs. temperature for large grains can be obtained by mapping the analogous curve for olivine into a new temperature range where each temperature is multiplied by a factor of 1.77. The actual calculated recombination efficiency for amorphous carbon is shown in Fig. 2, where it can be seen that the range

of high efficiency is indeed 11–16 K, as roughly expected from the above analysis and also from the master equation results, discussed but not plotted by Biham et al. (2001). Our results for both olivine and carbon differ from models 2 and 3 of Cazaux & Tielens (2004) (see their Fig. 15), where the existence of chemisorption sites can allow for moderate efficiencies at temperatures of up to 600 K.

For the models of homogeneous olivine and amorphous carbon surfaces considered here, we see that there are only small differences (up to a factor of a few) among the results of the stochastic approaches for recombination efficiency as a function of temperature. In general, if a factor of a few accuracy is all that is required for astronomical models, the agreement between approaches is sufficiently good that the master equation method is certainly an adequate approach to use in models for all grain sizes. On the other hand, both methods show that perfectly homogeneous surfaces of olivine and carbon with sites of weak binding only are unreasonable candidates for interstellar grain surfaces in low temperature regions because the efficient formation of molecular hydrogen is limited to unphysically narrow ranges of temperature, which also tend to be below the surface temperature of grains in diffuse interstellar clouds. So, let us consider inhomogeneous and mixed surfaces.

3.2. Inhomogeneous olivine and carbon surfaces

We now study how the recombination efficiency changes when the single desorption energy and diffusion barrier for atomic hydrogen on homogeneous olivine and amorphous carbon are replaced by distributions. Once again the case of olivine is emphasized. These distributions can represent olivine in the laboratory, since the observed breadth of the TPD spectral peaks is not fitted well by the single energies so far determined (Biham, private communication). More importantly, they can pertain to the poorly characterized surfaces of interstellar dust particles.

Figure 3 shows the recombination efficiency for standard type 1 grains ($316 \times 316 \approx 10^5$ sites) with a surface temperature of 10 K as a function of a measure of the width of both exponential and Gaussian distributions. This measure, known as the normalized variance and designated $\bar{\sigma}$, is defined as T_0/\bar{E}_b , where T_0 is the standard deviation for the Gaussian distribution and the average deviation from the lowest value for the exponential distribution, while \bar{E}_b is the average diffusion barrier. Since the desorption energy and diffusion barrier are defined to be correlated, their ratio is constant, and $\bar{\sigma}$ is the same for the desorption energy distributions. The parameters for the calculation are the same as before except that the single diffusion barrier and desorption energies for olivine have been converted into average values of 287 K and 373 K. To get a feel for the exponential distribution, consider a value of $\bar{\sigma} = 0.1$. Then, for the diffusive case, $T_0 = 28.7$ K and E_{b0} , the lowest barrier considered, is $287 \text{ K} - 28.7 \text{ K} = 258.3$ K. From the results in Fig. 3, we can clearly see that the efficiency of recombination increases dramatically with increasing $\bar{\sigma}$ for both exponential and Gaussian distributions. This is especially true for $\bar{\sigma}$ greater than 0.04. When the normalized variance reaches 0.1,

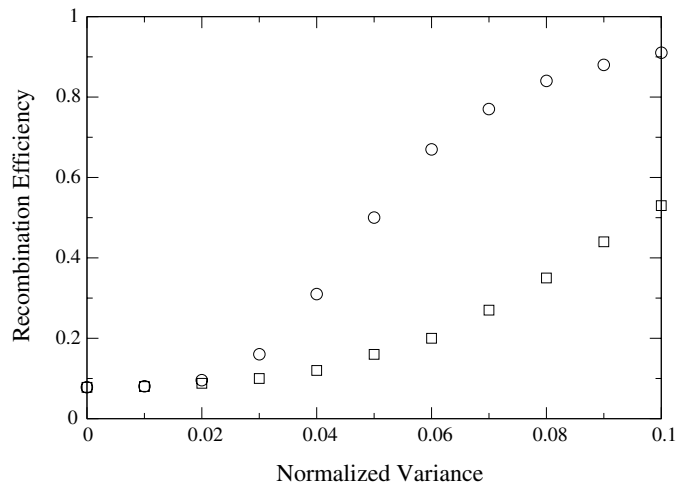


Fig. 3. Recombination efficiency as a function of $\bar{\sigma}$, the normalized variance, for standard type 1 olivine grains at 10 K. The circles are for an exponential distribution while the squares are for a Gaussian distribution.

the efficiency approaches unity for the exponential distribution and 0.55 for the Gaussian distribution. At the present time, it is not known what a reasonable value of $\bar{\sigma}$ might be for olivine. What limited information available is for H atoms and H₂ molecules on amorphous and low density water ices, which are probably more complex than olivine and amorphous carbon. The calculation of Buch & Czerminski (1991) on model clusters shows irregular but continuous distributions with $\bar{\sigma}$ in the vicinity of 0.3. An experimental TPD study soon to be published regarding D₂ desorption from ASW shows a very broad but irregular distribution of energies (Hornekaer et al., preprint). Another study (Perets et al. 2004) mentions the need for Gaussian distributions to model TPD data on low-density ice (LDI) without specifying their widths.

In addition to the efficiency of H₂ formation, a related result that is strongly dependent on the normalized variance is the number of H atoms present on the grain at steady-state, which is plotted in Fig. 4 vs. time (s) using values of $\bar{\sigma}$ ranging from 0.04 to 0.1. Note that, once steady state is reached, the number of hydrogen atoms is not fixed but shows random deviations. The number of H atoms on the surface clearly increases dramatically with increasing $\bar{\sigma}$ for the exponential distribution, reaching ≈ 300 at the highest $\bar{\sigma}$ studied. For a Gaussian distribution, a similar pattern happens except that the recombination efficiency and number of H atoms grow more slowly with increasing $\bar{\sigma}$. For example, with $\bar{\sigma} = 0.1$, the number of H atoms oscillates around 40, rather than 300. Figure 4 also depicts the time to reach steady state, which clearly depends on $\bar{\sigma}$. With $\bar{\sigma}$ near 0, steady state is reached after a few H atoms land on the grain, while for $\bar{\sigma} = 0.1$ and an exponential distribution, steady state is reached by 5×10^6 s.

In order to determine why both the recombination efficiency and the number of H atoms increase dramatically with increasing $\bar{\sigma}$, we studied the waiting times for the hopping and desorption of specific atoms when $\bar{\sigma} = 0.1$ on an olivine surface at 10 K. As expected, a wide range of waiting times is generated compared with that for the pure olivine surface, on

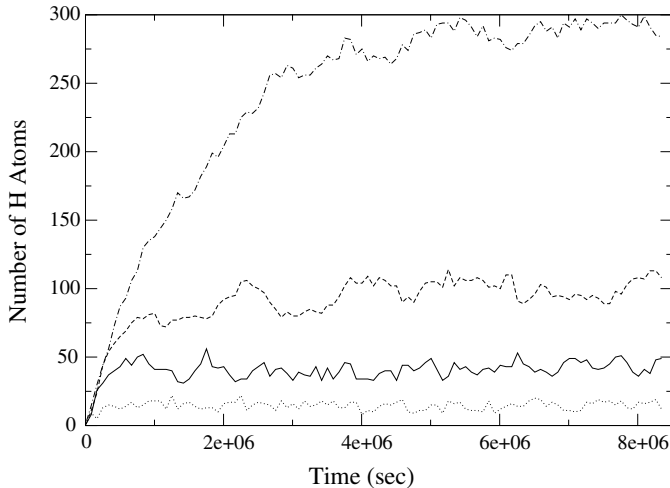


Fig. 4. The number of H atoms on a standard type 1 olivine grain at 10 K with assorted distributions of diffusion barriers possessing different values of $\bar{\sigma}$ is plotted versus time. Results for exponential distributions with $\bar{\sigma}$ of 0.04, 0.07, and 0.1 are depicted by dotted lines, dashed lines, and dashed-dotted lines, respectively. The solid line is for a Gaussian distribution with $\bar{\sigma} = 0.1$.

which the range of waiting times is rather small. Atoms with long waiting times remain stationary but available as reactant partners while atoms with short waiting times move quickly to other sites until they desorb, react, or find a site associated with a long waiting time. The net result is an increase in reaction efficiency.

Figure 5 shows the temperature dependence of the recombination efficiency for H_2 formation on standard olivine and amorphous carbon grains with both the exponential and Gaussian distributions, a type 1 lattice, and $\bar{\sigma}$ set to 0.1. It is obvious by comparison with Fig. 2 that high efficiencies, especially for the exponential distribution, extend to higher temperatures than for homogeneous grains. The reasons are similar to the reasons discussed for the enhanced efficiency at 10 K. On the other hand, high efficiencies do not extend significantly to lower temperatures because of the lack of mobility of H atoms with even small waiting times. The high efficiency for olivine, however, only extends to 10–12 K, depending upon the type of distribution, which is a significantly lower temperature than estimated for grain surfaces in diffuse clouds. More specifically, the upper temperature at which the efficiency is about 0.1 is 12.3 K for the exponential distribution and 10.6 K for the Gaussian distribution when $\bar{\sigma} = 0.1$.

The case of amorphous carbon is rather analogous to that of olivine. As with the homogeneous surfaces, recombination efficiency plots from the case of olivine can be mapped into the case of amorphous carbon by multiplying the temperature by 1.77. For example, the upper temperature at which the efficiency is 0.1 for a standard type 1 amorphous carbon grain with an exponential distribution and $\bar{\sigma} = 0.1$ would be expected to be $1.77 \times 12.3 \text{ K} = 21.8 \text{ K}$, which is significant because it is a high enough surface temperature to be representative of diffuse clouds. Our actual calculation shows this temperature to be 21.6 K. The analogous temperature for a Gaussian distribution with the same variance is 18.7 K. The lower temperature

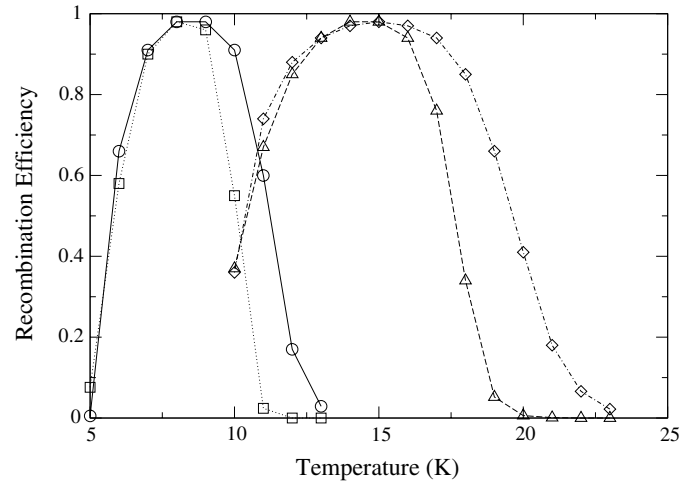


Fig. 5. Recombination efficiency on standard inhomogeneous olivine and amorphous carbon grains as a function of temperature with $\bar{\sigma} = 0.1$. For olivine, circles represent results for an exponential distribution while squares represent results for a Gaussian distribution. For amorphous carbon, diamonds represent results for an exponential distribution while triangles represent results for a Gaussian distribution.

at which the efficiency is 0.1 moves downward slightly from the homogeneous case. Inhomogeneous amorphous carbon is then a more attractive candidate as a surface for H_2 formation in diffuse clouds but one must remember that carbon grains are probably a minority population given that they may be formed only in carbon-rich AGB stars. So it is useful to study mixed olivine-carbon structures.

The efficiencies studied so far for inhomogeneous olivine are for grains in the asymptotic limit. We also would like to see how the recombination efficiency decreases when the grain size decreases. Rather than performing this study at 10 K, as was done for homogeneous olivine, we choose a temperature at which the asymptotic large-grain recombination efficiency is approximately the same; i.e., approximately 0.1. Figure 6 shows the size dependence of the recombination efficiency for type 1 grains and $\bar{\sigma} = 0.1$ using an exponential distribution at 12.3 K and a Gaussian distribution at 10.6 K, at which the asymptotic recombination efficiency is indeed 0.1. It is clear that, analogous to the homogeneous olivine surface, the recombination efficiency drops when the grain size is very small, but here the diminution appears to require far smaller grain sizes to be significant. The smaller the grain size, however, the greater the uncertainty due to the diversity of grain surfaces. Error bars representing one standard deviation are shown in Fig. 6, where it can be seen that they are large enough to weaken the case for size dependence.

3.3. Surfaces composed of olivine and carbon mixtures

3.3.1. Mixed surfaces with randomly distributed carbon

We first report results for mixed surfaces between homogeneous olivine and homogeneous amorphous carbon in which the carbon atoms are distributed randomly. Figure 7 shows

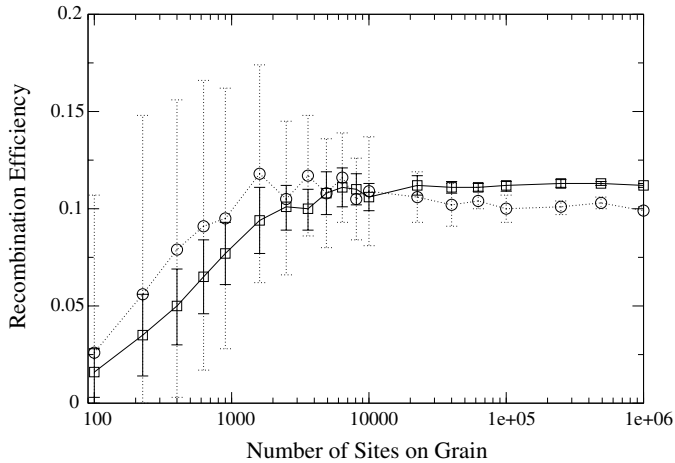


Fig. 6. Recombination efficiency on inhomogeneous olivine grains as a function of grain size for $\bar{\sigma} = 0.1$. The circles are for an exponential distribution at a temperature of 12.3 K while the squares are for a Gaussian distribution at a temperature of 10.6 K. Error bars represent one standard deviation. The non-zero standard deviation is caused by the diversity of surfaces, all of the same size but differing in the randomly-chosen pattern of diffusive barriers and binding energies.

the recombination efficiency as a function of temperature for type 1 standard mixed olivine-carbon grains with 1.8%, 20%, and 40% carbon. On these surfaces, there are, respectively, 1800, 20 000 and 40 000 randomly placed carbon atoms. Looking at the results qualitatively, we see that the range of high efficiencies for olivine-carbon mixtures encompasses the narrower ranges for the pure substances (Fig. 2) plus the temperatures in between these ranges. A closer look shows that the mixed olivine-carbon surfaces show efficiencies that decrease with increasing temperature a little more rapidly than pure carbon. Specifically, the upper temperature for the 1.8% carbon surface at which the efficiency drops to 0.1 is 13.7 K, while for the 20% carbon surface, it is 14.5 K, and for the 40% carbon, 14.9 K. The analogous value for pure amorphous carbon is about 17.4 K.

The size dependence of the recombination efficiency is shown in Fig. 8 for type 1 lattices with 1.8% and 40% carbon. As with inhomogeneous olivine, the temperatures are chosen on the high end of the peak efficiency when the asymptotic efficiency is near 0.1. Once again, in analogy with the inhomogeneous olivine surface, the size dependence is weak compared with homogeneous surfaces. In this case, there is no uncertainty associated with diverse structures since there are no distributions.

3.3.2. Mixed surfaces with carbon clusters

We have simulated the effect of islands (Kolasinski 2002) on standard grains at two carbon-olivine compositions. For a grain with 1.8% carbon (1800 atoms), we randomly deposit eight islands of $15 \times 15 = 225$ carbon atoms each while for a grain with $\approx 40\%$ carbon (39 690 atoms), we randomly deposit ten islands of $63 \times 63 = 3969$ atoms. The recombination efficiencies as functions of temperature show some differences from those for random carbon atom deposition, as shown in Fig. 9.

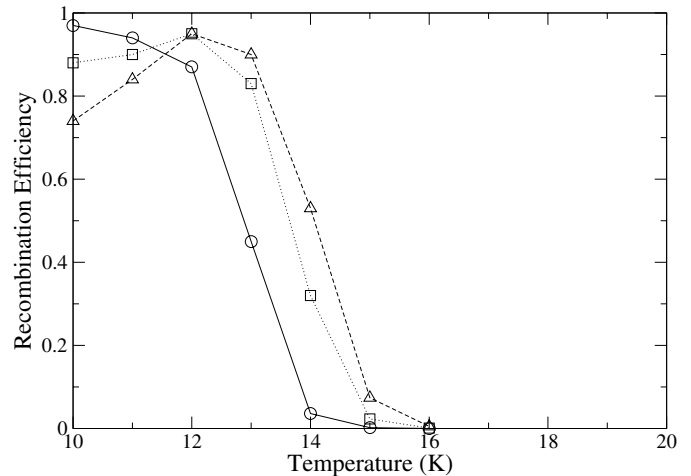


Fig. 7. Recombination efficiency as a function of temperature for standard carbon-olivine grains of type 1. The circles are for 1.8% carbon, the squares for 20% carbon, and the triangles for 40% carbon.

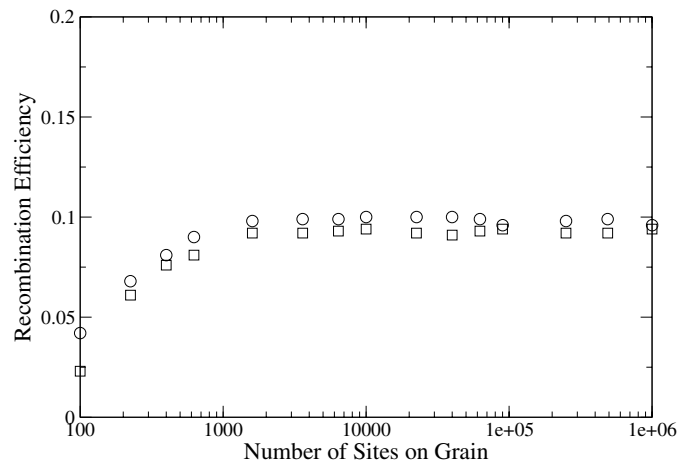


Fig. 8. Recombination efficiency for carbon-olivine grains as a function of size for grains of type 1. The squares are for 1.8% carbon at 13.7 K, and the circles are for 40% carbon at 14.9 K.

For the 1.8% carbon surface, the efficiency drops to about 0.1 at 12.8 K, a somewhat lower temperature than for the analogous random case, while for the 40% carbon surface, the analogous temperature is 15.8 K, a somewhat higher temperature than for the analogous random case. It is difficult to simulate the size dependence of this type of surface because if we change the lattice size, we have to change the carbon island size or distance between islands to maintain the same percentage of carbon.

3.3.3. Mixed surfaces with randomly distributed and inhomogeneous carbon

Here we initially assume exponential and Gaussian distributions with $\bar{\sigma} = 0.1$ for the H atoms that bind at carbon sites, while a single diffusion barrier and desorption energy exist for the olivine sites. (The even more complex case that also includes inhomogeneous olivine will not strongly affect the results.) The average carbon diffusion barrier and desorption energy are equal to the values for pure homogeneous amorphous

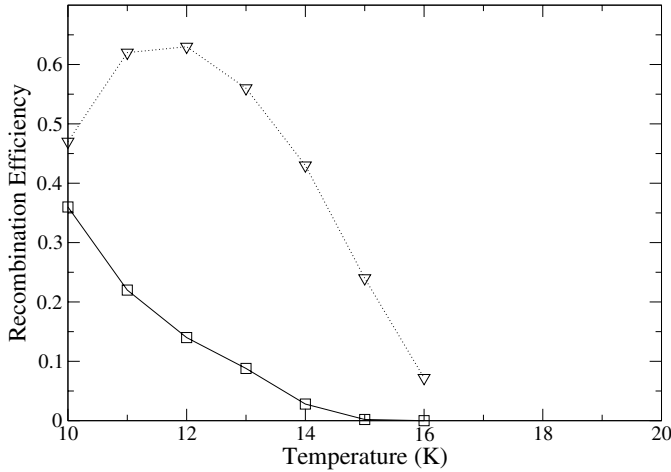


Fig. 9. Recombination efficiency as a function of temperature for standard carbon-olivine grains of type 1 with 1.8% and 40% carbon, but localized into islands. Results with the lower percentage are illustrated with squares, while results with the higher percentage are illustrated with downward triangles.

carbon. Again, we force the desorption energy and diffusion barrier for H atoms on carbon sites to be correlated. Figure 10 shows the temperature dependence of the recombination efficiency for standard grains of type 1 with 40% of the lattice sites carbon. The recombination efficiency is found to remain high at temperatures from below 10 K to 18 K for an exponential distribution and to 16 K for a Gaussian distribution – the recombination efficiency drops to 0.1 at 18.1 K and 16.4 K, respectively, for the two distributions. Since the surface being considered is rather complex in nature, we have felt justified in rerunning the calculations with $\bar{\sigma}$ raised to 0.2; the results are also shown in Fig. 10. Now the temperature at which the efficiency drops to 0.1 rises to 21.6 K for the exponential distribution and to 18.8 K for the Gaussian distribution.

We have also studied the size dependence of the recombination efficiency when $\bar{\sigma} = 0.2$, which is shown in Fig. 11 for temperatures at which the recombination efficiency has dropped to 0.1. It can be seen that the efficiency is almost totally independent of size until the very small size of 100 lattice sites is reached. So, even small grains of this composition and inhomogeneity are efficient at producing H₂. Of course, the uncertainty in our results for small grains is once again large because of the diversity among different samples.

3.3.4. Mixed surfaces with clustered and inhomogeneous carbon

Figure 12 shows the recombination efficiency vs. temperature for standard mixed olivine-carbon grain surfaces of type 1 for $\bar{\sigma} = 0.2$ with $\approx 40\%$ of the lattice consisting of carbon in clusters of 63×63 sites. In this figure, it can be seen that the regime of high efficiency extends to even higher temperatures: the recombination efficiency drops to 0.1 at 23.8 K and 19.9 K for the exponential and Gaussian distributions, respectively.

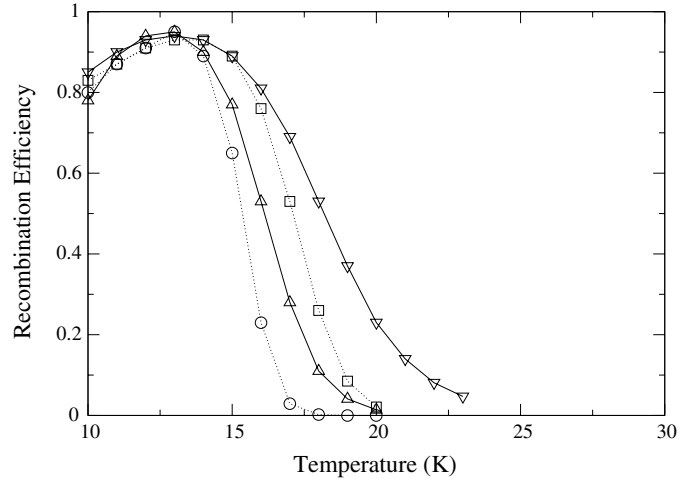


Fig. 10. Recombination efficiency vs. surface temperature for standard type 1 olivine-carbon grains with 40% of the lattice sites occupied by randomly placed carbon atoms. The carbon diffusion barrier and desorption energy follow distributions with $\bar{\sigma} = 0.1$ and 0.2. Upward triangles are used for the exponential distribution with the lower variance, downward triangles are used for the exponential distribution with the higher variance, circles are used for the Gaussian distribution with the lower variance, and squares are used for the Gaussian distribution with the higher variance.

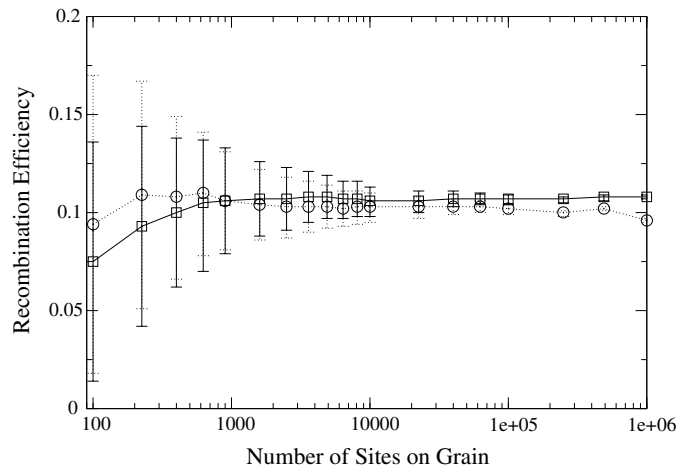


Fig. 11. Recombination efficiency vs. size for standard type 1 olivine-carbon grains with 40% of the lattice sites occupied by randomly placed carbon atoms. The carbon diffusion barrier and desorption energy follow distributions with $\bar{\sigma} = 0.2$. The circles are for an exponential distribution at 21.6 K while the squares are for a Gaussian distribution at 18.8 K. Error bars represent one standard deviation. The standard deviation arises from diverse grains of the same size but different patterns of diffusive barriers and binding energies.

4. Summary and conclusions

A Monte Carlo simulation based on the continuous-time random walk approach (CTRW) of Montroll & Weiss (1965) has been used to study the efficiency of H₂ formation on cold interstellar grains. The approach involves viewing the surface of a grain as a square lattice with periodic boundary conditions. The adsorption, desorption, and hopping of H atoms on the lattice are followed, and a reaction efficiency is calculated once the

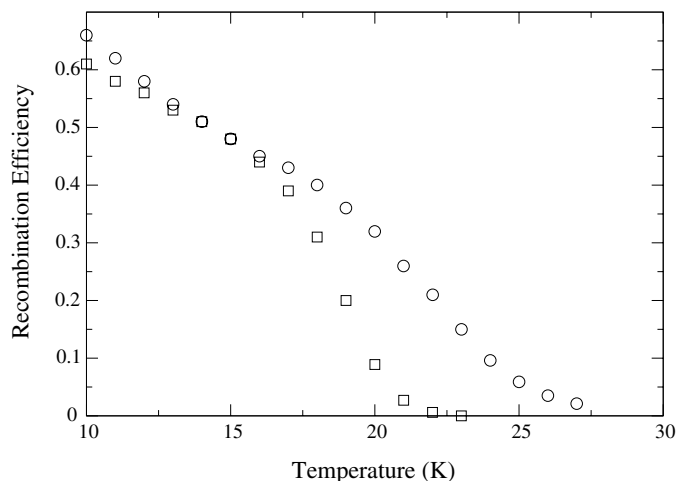


Fig. 12. Same as Fig. 10 except that the carbon is in the form of islands and only results for $\bar{\sigma} = 0.2$ are plotted. The circles are for an exponential distribution while squares are for a Gaussian distribution.

system reaches a steady state. Our calculations are meant to pertain to conditions in diffuse interstellar clouds, where a significant amount of interstellar molecular hydrogen is produced on granular surfaces.

Although the CTRW approach can be used to study homogeneous grain surfaces with single values for the diffusive barrier and desorption energy of hydrogen atom adsorbates, it is perhaps most useful for more complex surfaces. Since infra-red spectra indicate strongly that interstellar grains are amorphous rather than crystalline, it is exceedingly unlikely that only a single diffusive barrier and binding energy for atomic hydrogen pertain for realistic surfaces. Yet the widths of distributions of these barriers and energies are highly uncertain, so that no single width can be regarded as representative. Moreover, it is also possible that surfaces of grains in diffuse interstellar clouds are chemically inhomogeneous, although without knowledge of the details of grain formation, it is again difficult to decide what chemical make-up is most representative.

For homogeneous surfaces, the CTRW approach is more exact than other methods, including stochastic ones such as the master equation approach (Biham et al. 2001; Green et al. 2001), because it includes consideration of back diffusion into previously occupied lattice sites, a consideration that can lower the reaction efficiency for large grains at temperatures above peak efficiency. At these temperatures, as homogeneous grains become sufficiently small that, on average, there is less than 1 hydrogen atom per grain, the efficiency of H_2 formation decreases significantly according to master equation calculations but not rate equation calculations, which always mistakenly yield the asymptotic limit for large grains. Our results show the same qualitative effect as the master equation approach but the efficiency decreases more slowly with decreasing grain size such that eventually the two methods coalesce. At temperatures where the reaction efficiency is quite high, there is little size dependence.

We have considered three types of more complex granular surface structures: (i) pure (“inhomogeneous”) surfaces in which the diffusive barrier and desorption energy for H atoms

on the surface follow probability distributions that are either exponential or Gaussian, with a normalized variance $\bar{\sigma}$ to indicate the ratio of the breadth to the mean value of the distribution; (ii) surfaces composed of specific mixtures of homogeneous olivine and homogeneous amorphous carbon in which the carbon atoms are inserted in random single positions or islands in the lattice; and (iii) mixed olivine-carbon grains in which the inhomogeneous carbon sites possess a distribution of diffusive barriers and desorption energies.

The results of our many calculations on type 1 lattices (four nearest neighbors) are summarized in Table 1, where we list the surfaces studied, the type of distribution used for diffusive barriers and desorption energies (if applicable), the normalized variance $\bar{\sigma}$ of the distributions, the so-called “asymptotic lattice size”, which is the minimum size to reach the asymptotic efficiency limit at $T_{0.1}^{\text{up}}$ (K), the temperature where the recombination efficiency drops from its peak at lower temperatures to 0.1 for standard lattices of 10^5 sites, and the time t_{ss} (s) taken to reach steady state conditions for grains of this size and temperature. Note that an entry “NA” stands for “non-applicable”. We have emphasized the upper range of temperatures to which recombination remains efficient because the homogeneous olivine and amorphous carbon considered earlier (Katz et al. 1999) possess high efficiencies only at surface temperatures below those estimated for diffuse clouds. Moreover, the calculation of efficiencies at the lower range of temperatures is rendered difficult by a variety of problems including the need to consider non-thermal ejection of H_2 product and whether the Eley-Rideal mechanism plays a role when surface H atoms are unable to hop. All surfaces considered are calculated to be efficient producers of H_2 down to temperatures of 11 K (homogeneous carbon) or lower, with homogeneous olivine efficient down to 6 K.

In qualitative agreement with other approaches (Katz et al. 1999; Biham et al. 2001), we find narrow distributions of high reaction efficiency for homogeneous olivine and amorphous carbon. Table 1 shows that if we adopt distributions of diffusion barriers and desorption energies, the temperature range for efficient H_2 formation increases by spreading out to higher temperature, presumably because a fraction of H atoms are trapped in deep binding wells and await the approach of other H atoms to form molecules. The effect increases for increasing values of the normalized variance $\bar{\sigma}$. For the same normalized variance, the exponential distribution produces the greater effect, probably since the Gaussian distribution possesses too many sites with artificially low barriers and desorption energies. If we utilize a sizeable normalized variance of 0.2, we find that $T_{0.1}^{\text{up}}$ reaches high values for a variety of inhomogeneous grains. For example, it is 23.8 K for a mixed olivine-carbon grain in which the carbon atoms lie in clusters with an exponential distribution for diffusive barriers and desorption energies.

Two other factors distinguish the inhomogeneous and mixed surfaces from the homogeneous surfaces at temperatures above peak efficiencies: (i) the size dependence of the recombination efficiency is much weaker albeit uncertain for the inhomogeneous case due to the diversity of surface diffusive and binding energies; and (ii) the time taken to reach steady state increases because of, among other reasons, the larger number

Table 1. Summary of results on type 1 surfaces.

Surface	Distribution	$\overline{\sigma}$	Asymptotic size (sites)	$T_{0.1}^{\text{up}}$ (K)	t_{ss} (s)
Homogeneous Olivine	NA	0	1×10^4	9.9	10^{3-4}
Homogeneous Carbon	NA	0	1×10^4	17.4	10^{3-4}
Inhomogeneous Olivine	Exponential	0.1	1000	12.3	10^5
Inhomogeneous Olivine	Gaussian	0.1	5000	10.6	10^4
Inhomogeneous Carbon	Exponential	0.1	1000	21.6	10^5
Inhomogeneous Carbon	Gaussian	0.1	4000	18.7	10^4
Random Olivine-Carbon	NA	0	900	13.7	10^5
1.8% Carbon					
Random Olivine-Carbon	NA	0	900	14.5	10^5
20% Carbon					
Random Olivine-Carbon	NA	0	900	14.9	10^5
40% Carbon					
Clustered Olivine-Carbon	NA	0	NA	12.8	5×10^6
1.8% Carbon					
Clustered Olivine-Carbon	NA	0	NA	15.8	10^5
40% Carbon					
Random Olivine-Carbon	Exponential	0.1	200	18.1	2×10^6
40% Carbon					
Random Olivine-Carbon	Gaussian	0.1	900	16.4	8×10^5
40% Carbon					
Random Olivine-Carbon	Exponential	0.2	100	21.6	5×10^7
40% Carbon					
Random Olivine-Carbon	Gaussian	0.2	400	18.8	3×10^6
40% Carbon					
Clustered Olivine-Carbon	Exponential	0.2	NA	23.8	1×10^7
40% Carbon					
Clustered Olivine-Carbon	Gaussian	0.2	NA	19.9	3×10^6
40% Carbon					

of H atoms resident on the surface. The first factor means that small grains may play a greater role in the formation of H_2 if inhomogeneous materials are the better representation of interstellar grains. Of course, very small grains are subject to stochastic heating by photons, which will inhibit the efficiency of H_2 formation by driving H atoms off of the grains (Draine & Li 2001; Li & Draine 2001).

Based on the results of this work, it appears that sufficiently inhomogeneous surfaces on interstellar grains allow a high enough efficiency over a wide enough range of temperatures and grain sizes to explain the formation of H_2 in diffuse interstellar clouds. To achieve efficient molecular hydrogen formation on even warmer grains, such as occur in photon-dominated regions, one can include sites with greater amounts of binding energy such as those with chemisorption (Cazaux & Tielens 2004). Such “binary” systems have heretofore been studied to date only with rate equations, although it should be simple to extend our approach to study them and to include distributions of energies. Another possibility is to extend the

normalized variance of our current model lattices to rather high values. For such high values of $\overline{\sigma}$, we use only an exponential distribution because of the problem that the Gaussian distribution can include negative energies. If we, for example, use a normalized variance of 0.5 with an exponential distribution for standard type 1 lattices, we obtain values for $T_{0.1}^{\text{up}}$ of 20.0 K, 35.1 K, 29.0 K, and 30.2 K, respectively, for olivine, amorphous carbon, mixed olivine – carbon (40%, random sites) and mixed olivine-carbon (40%, islands). For comparison, it is to be noted that surface temperatures for large grains in PDR’s are thought to range from 15 K (Chameleon) through 90 K (Orion bar) (Habart et al. 2004). It will be interesting to see if future laboratory investigations on complex surfaces can determine proper normalized variances for astrochemists to utilize.

After this paper was substantially finished, we learned of new Monte Carlo calculations on surface H_2 formation by Dr. S. Cazaux (Arcetri).

Acknowledgements. We acknowledge the careful reading by the referee of the initial version of this manuscript. E.H. acknowledges the

support of the National Science Foundation (US) for his research program in astrochemistry. We thank the Ohio Supercomputer Center for computer time on their SV1 machine.

References

- Bedeaux, D., Lakatos-Lindenberg, K., & Shuler, K. E. 1971, *J. Math. Phys.*, 12, 2116
- Biham, O., & Lipshtat, A. 2002, *Phys. Rev. E*, 66, 056103
- Biham, O., Furman, I., Pirronello, V., & Vidali, G. 2001, *ApJ*, 553, 595
- Buch, V., & Czermanski, R. 1991, *J. Chem. Phys.*, 95, 6026
- Caselli, P., Hasegawa, T. I., & Herbst, E. 1998, *ApJ*, 495, 309
- Caselli, P., Stantcheva, T., Shalabiea, O., Shematovich, V. I., & Herbst, E. 2002, *Planet. Space Sci.*, 50, 1257
- Cazaux, S., & Tielens, A. G. G. M. 2004, *ApJ*, 604, 222
- Charnley, S. B. 2001, *ApJ*, 562, L99
- Draine, B. T., & Li, A. 2001, *ApJ*, 551, 807
- Duley, W. W., & Williams, D. A. 1984, *Interstellar Chemistry* (London: Academic)
- Gillespie, D. T. 1976, *J. Comp. Phys.*, 22, 403
- Gould, R. J., & Salpeter, E. E. 1963, *ApJ*, 138, 393
- Green, N. J. B., Toniazzo, T., Pilling, M. J., et al. 2001, *A&A*, 375, 1111
- Habart, E., Boulanger, F., Verstraete, L., Walmsley, C. M., & Pineau des Forêts, G. 2004, *A&A*, 414, 531
- Hasegawa, T. I., Herbst, E., & Leung, C. M. 1992, *ApJS*, 82, 167
- Herbst, E. 2001, *Chem. Soc. Rev.*, 30, 168
- Hinrichsen, H. 2000, *Adv. Phys.*, 49, 7
- Hornekaer, L., Baurichter, A., Petrunin, V. V., Field, D., & Luntz, A. C. 2003, *Science*, 302, 1943
- Katz, N., Furman, I., Biham, O., Pirronello, V., & Vidali, G. 1999, *ApJ*, 522, 305
- Kolasinski, K. W. 2002, *Surface Science* (West Sussex: Wiley)
- Krug, J. 2003, *Phys. Rev. E*, 67, 065102
- Li, A., & Draine, B. T. 2001, *ApJ*, 554, 778
- Lin, A., Kopelman, R., & Argyrakis, P. 1996, *Phys. Rev. E.*, 53, 1502
- Lindenberg, K., Argyrakis, P., & Kopelman, R. 1995, *J. Phys. Chem.*, 99, 7542
- Lipshtat, A., & Biham, O. 2004, PRL, submitted
- Lipshtat, A., Biham, O., & Herbst, E. 2004, *MNRAS*, 348, 1055
- Montroll, E. W., & Weiss, G. H. 1965, *J. Math. Phys.*, 6, 167
- Perets, H. B., Biham, O., Pirronello, V., et al. 2004, *ApJ*, submitted
- Pickles, J. B., & Williams, D. A. 1977, *Ap&SS*, 82, 167
- Pirronello, V., Biham, O., Liu, C., Shen, L., & Vidali, G. 1997a, *ApJ*, 483, L131
- Pirronello, V., Liu, C., Shen, L., & Vidali, G. 1997b, *ApJ*, 475, L69
- Pirronello, V., Liu, C., Roser, J. E., & Vidali, G. 1999, *A&A*, 344, 681
- Roberts, H., & Herbst, E. 2002, *A&A*, 395, 233
- Roser, J. E., Manicò, G., Pirronello, V., & Vidali, G. 2002, *ApJ*, 581, 276
- Sha, X., & Jackson, B. 2002, *Surf. Sci.*, 496, 318
- Simon, H. 1995, *J. Phys. A*, 28, 6585
- Stantcheva, T., & Herbst, E. 2004, *A&A*, 423, 241
- Stantcheva, T., Shematovich, V. I., & Herbst, E. 2002, *A&A*, 391, 1069
- Tielens, A. G. G. M., & Allamandola, L. J. 1987, in *Interstellar Processes*, ed. D. J. Hollenbach, & H. A. Thronson, Jr. (Dordrecht: Reidel), 397
- Tielens, A. G. G. M., & Hagen, W. 1982, *A&A*, 114, 245
- Watson, W. D., & Salpeter, E. E. 1972, *ApJ*, 174, 321
- Weiss, G. H., & Rubin, R. J. 1983, *Adv. Chem. Phys.*, 52, 363
- Williams, D. A. 1998, *Faraday Discuss.*, 109, 1
- Zecho, T., Guttler, A., Sha, X., Jackson, B., & Kuppers, J. 2002, *J. Chem. Phys.*, 117, 8486